On the Characteristics of Air-Bearing

By

Tokio SASAKI and Haruo MORI

Department of Mechanical Engineering

(Received Dec, 1950)

1. Introduction

Concerning the plain bearing lubricated with air, a series of experiments was carried out by Kingsbury in 1897 [1], and its theoretical analysis was then performed by Harrison in 1913 [2] by using the data of Kingsbury's experiments. In the above cases, however, the naturally-produced air film by the rotation of shaft was used. Concerning the cylindrical air-bearing in which the shaft is floated by the air injected through the nozzle under pressure, experiments and theoretical studies were made by Rokuro Sasaki in 1943 [3]. After that, we have developed the same subject with the systematic experiments and the theoretical consideration described in the following chapter.

2. Friction of Air-Bearing

In order to measurs the coefficient of friction, we have used thres methods ; damping method, pendulum method and balance beam method. Fig. 1 shows the damping method. The shaft S is fixed at both ends, and B is a bush pushed into the rotating disc D on the shaft S, from which the air is injected into the bearing clearance. Starting from the specified rotating speed, the returdation of rotation in free running state is measured by a stroboscopic method, and the coefficient of friction may be calculated from the damping ratio of the rotating speed. Pendulum method shown in Fig. 2 is as follows. The load W is hanged as a pendulum to the bearing B on the rotating shaft S. The frictional resistance

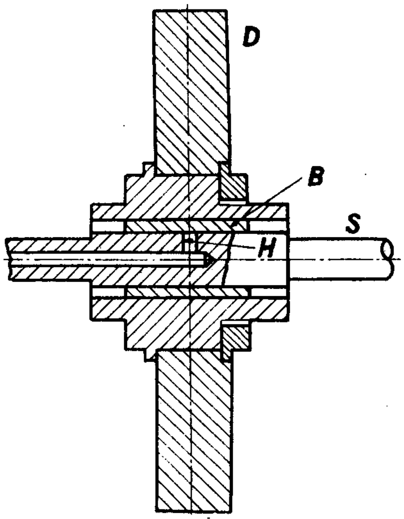

Fig. 1

can be calculated by the inclined angle of the pendulum measured by telescope and scale. In Fig. 2, M is a mirror fixed to the bearing, D is oil damper and T is rubber tube to supply air. Fig. 3 shows the balance beam method, in which the test bearing B is pushed inside of a holder carrying the balance beams with loading weight W on each side. Air is supplied from a nipple N and injected into the bearing clearance through a hole H. An index located in

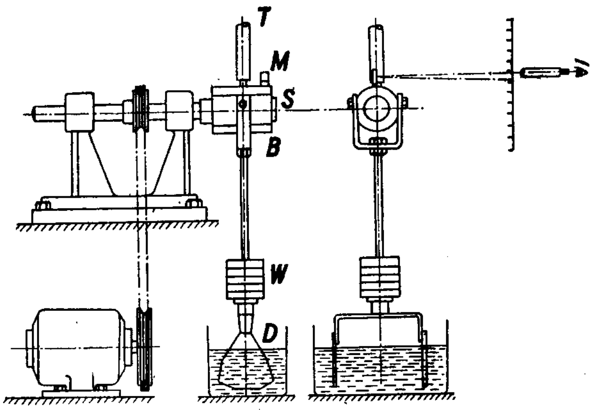

Fig. 2

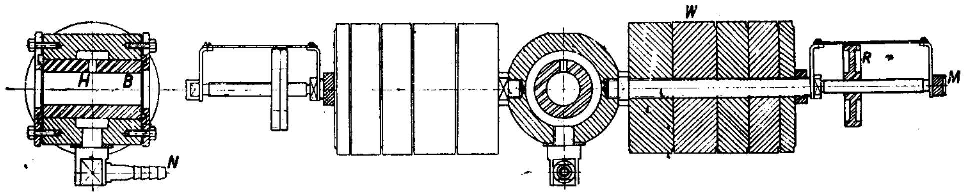

Fig. 3

front of light source is reflected by the mirror M at the end of beam and projects an image on the scale. R is a movable scaled-wheel sliding on the fine thread screw and the friction moment can be measured by adjusting the position of R and by forming the image of index at zero point of scale.

The results of the experiments are as follows: Concerning the coefficient of friction μ, the relations between the air supplying pressure p_0 (gage pressure) and the bearing clearance 2δ i. e. the difference of the inside diameter of the bush and the shaft diameter for various values of μ were measured at first by damping method, where rotating speed $n=200$ r. p. m., load $W=3.98$ kg, shaft diameter $d=20$ mm, bearing length $l=50$ mm and the various bearing clearances are 0.025, 0.035, 0.040, 0.060, 0.080 and 0.110 mm. These are shown in Fig. 4 and 5. In this test, two kinds of the air nozzle, radially bored nozzle shown as A in Fig. 6

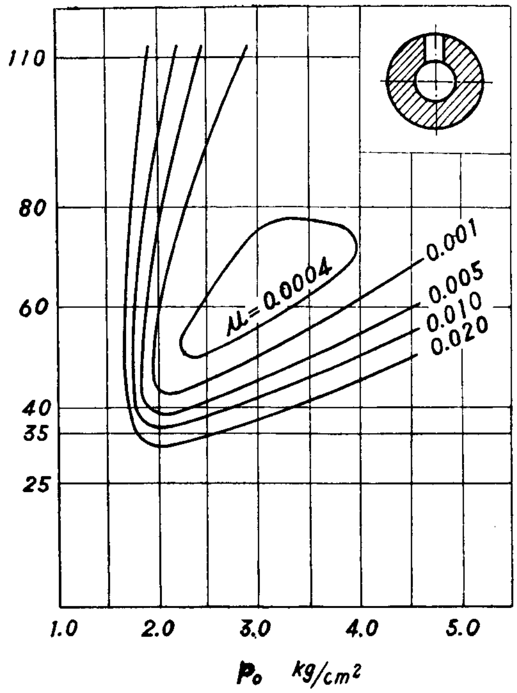

Fig. 4

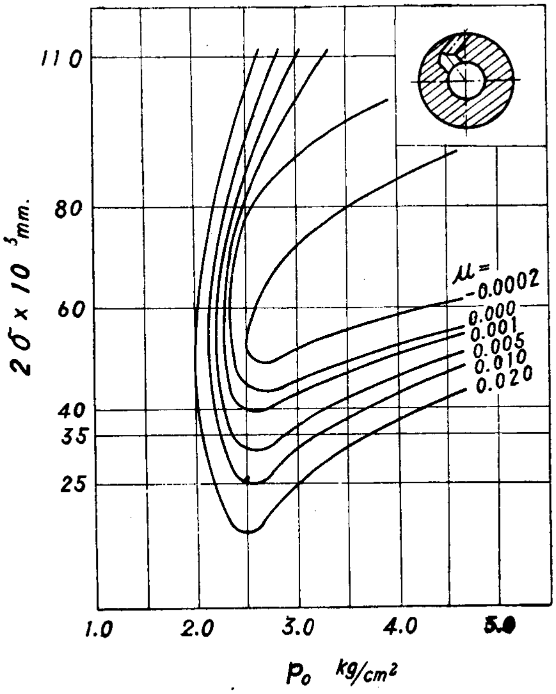

Fig. 5

and inclined nozzle shown as B, are used. Fig. 4 shows the results of experiment using the nozzle A, and Fig. 5 shows those using the nozzle B. In Fig. 5, it may be noticed that there is a region in which the coefficient of friction takes negative value showing the existence of motive force.

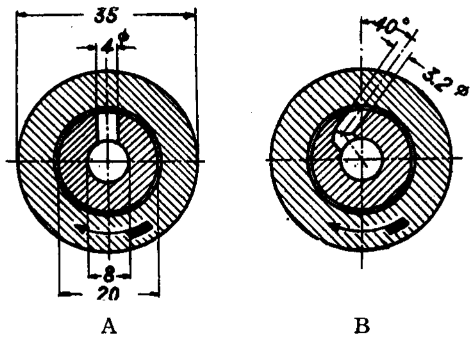

Fig. 6

The relations between μ, p_0 and W measured by balance beam method in which d=20 mm and the air nozzle bored radially are shown in Fig. 7. The coefficient of friction takes the minimum value for each bearing load, and these conditions give the most suitable air supplying pressure for the minimum friction of bearing. θ in Fig. 7, 9 and 10 is the angle of inclined air nozzle shown in Fig. 8. Fig. 9 shows the relation between the bearing load and the minimum coefficient of friction, in which, as the bearing load increases, μ_{min} decreases at first and then takes a constant value. Fig. 10 shows the relation between the bearing load W and p_{min}/q where p_{min} is air supplying pressure corresponding to μ_{min} and q is average bearing pressure $\frac{W}{ld}$.

Fig. 11 shows the relation of speed n and μ_{min} that is obtained by

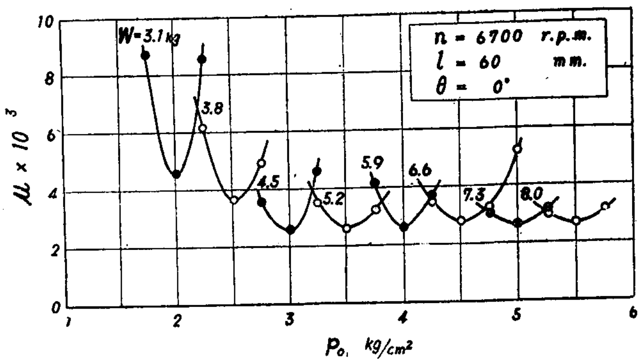

Fig. 7

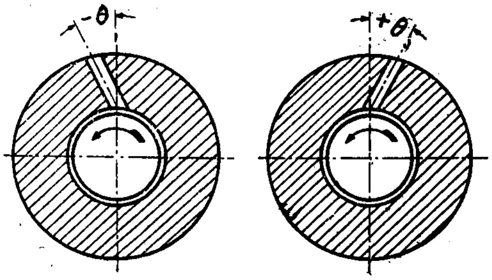

Fig. 8

pendulum method, in which we changed the bearing clearance to 0.070, 0.085 and 0.110 mm for a bearing of 30 mm in diameter, 75 mm in length. In this diagram, the frictional resistance increases linearly with the increase of speed for each bearing clearance, and it is supposed that the increase of friction owing to speed increment is caused by the viscous resistance of air-film. The influence of bearing clearance upon μ_{min} is shown in Fig. 12, and the relation between p_{min}/q and $2\,\delta$ is shown in Fig. 13.

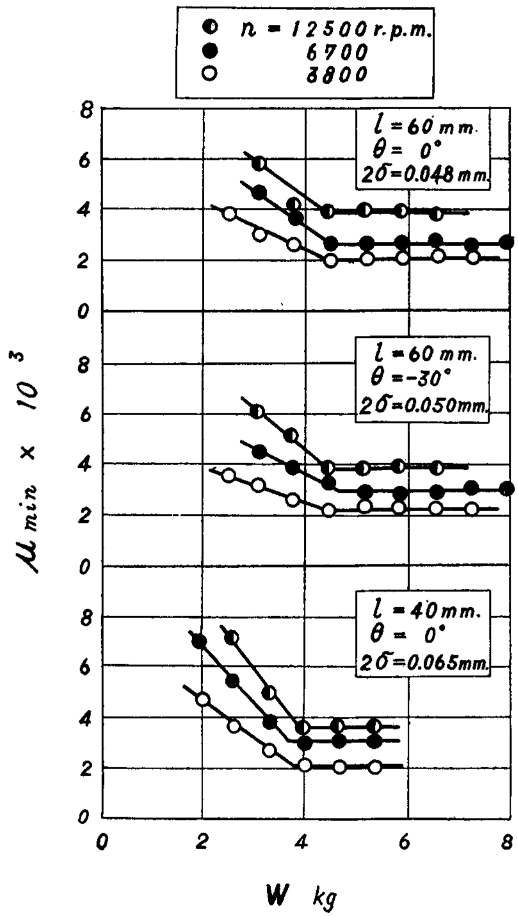

Fig. 9

As above described, the coefficient of friction of the air-bearing can be reduced into such small value as 10^{-3} order by adjusting air supplying pressure.

But when the same bearing is lubricated with spindle oil the friction is not so small as shown in Fig. 14.

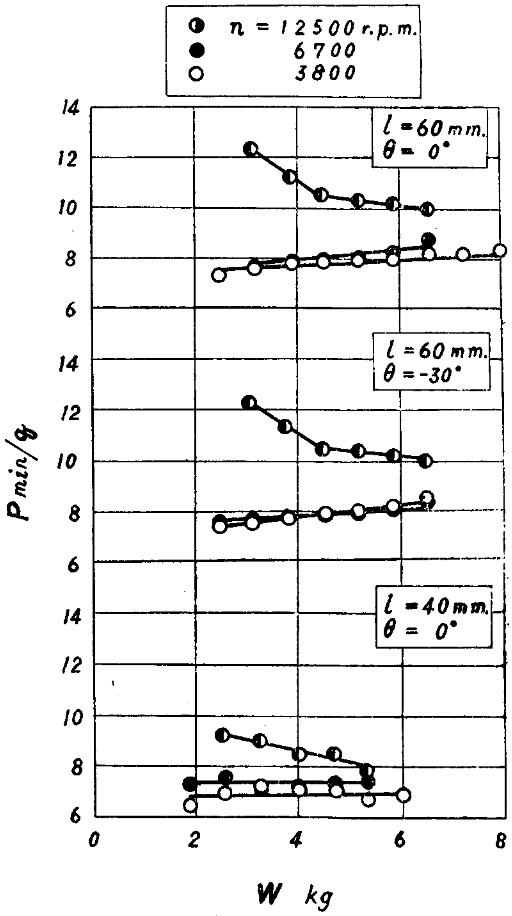

Fig. 10

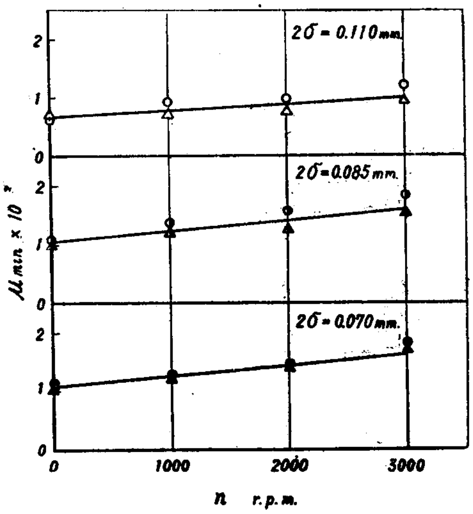

Fig. 11

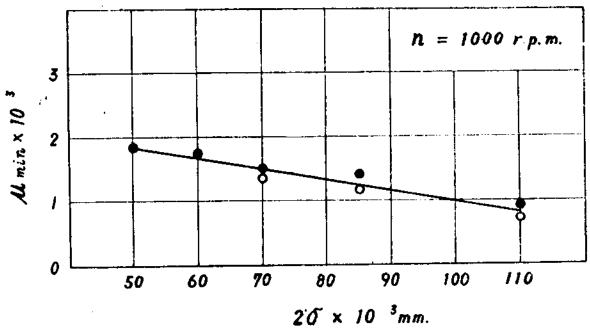

Fig. 12

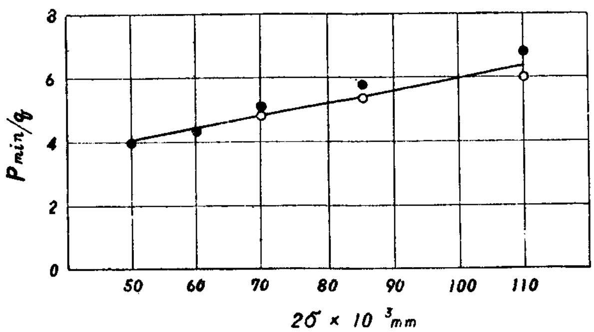

Fig. 13

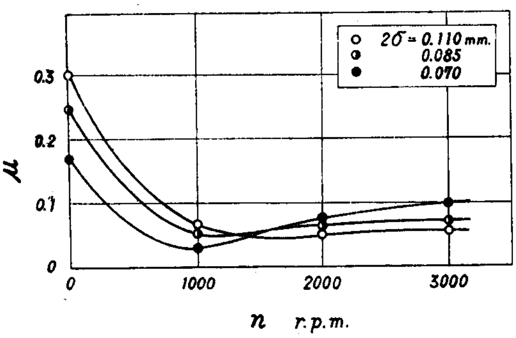

Fig. 14

3. Distribution of Pressure

As the pressure distribution in the bearing clearance is connected with the friction, pressures in the air–film were measured by a specimen shown in Fig. 15, measuring the friction moment at the same time by pendulum method. Two journals of 100 and 60 mm in length were used so that the influence of the bearing length might be inspected, and the bearing clearance of 0.110 mm and the bearing load of 9.1 Kg were used. The coefficient of friction and air supplying pressure have the tendencies as shown in Fig. 16 for the bearing length $l=100$ mm and $n=500$ r. p. m. in which the minimum friction is at $p_0=4.0$ Kg/cm²

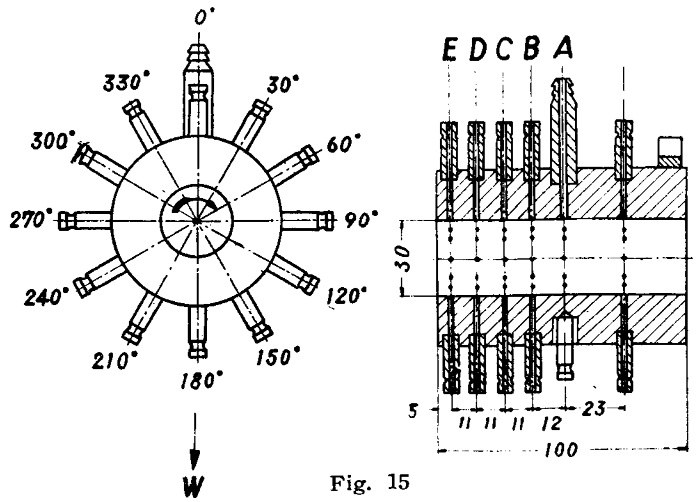

Fig. 15

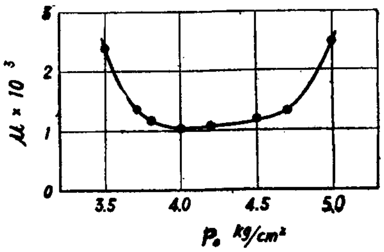

Fig. 16

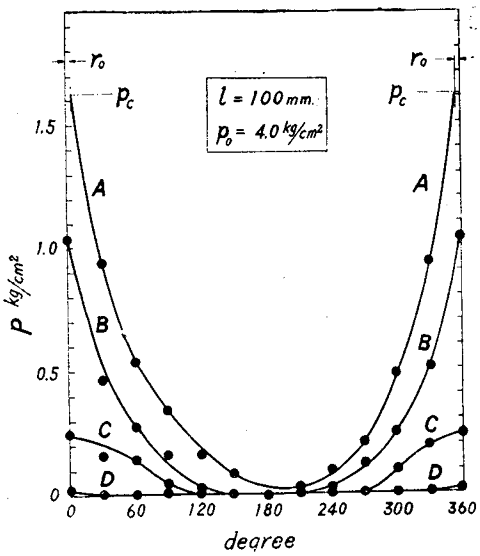

Fig. 17

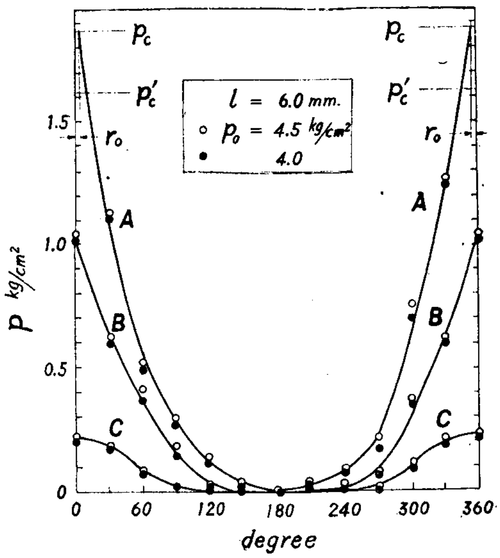

Fig. 18

(gage pressure). The distributions of pressure corresponding to the minimum friction for $l=100$ and 60 mm are shown in Fig. 17 and Fig. 18, in which r_0 is the radius of the air hole and p_c is the critical pressure. Comparing Fig. 17 and Fig. 18, the state of pressure distribution is nearly the same. These experiments were made under $n=0$, 500, 800 and 1300 r. p. m., but the variation of rotating speed did not effect the pressure distribution. And also, it was seen that the air pressure in the bearing near the air hole is far below the air supplying pressure. This fact means that the air pressure drops to the critical pressure p_c from p_0 at the inlet of bearing clearance and air flows into the bearing clearance at the sonic velocity.

4. Quantity of Flow

If the air flows as above mentioned, G, the quantity of flow, is given as follows, since the surface velocity of the shaft can be neglected as compared with the sonic velocity of air,

$$G = 2\pi r_0 \cdot h \cdot \frac{2}{3} a \cdot \gamma_e , \qquad (1)$$

where, r_0 is the radius of air hole, h is the bearing clearance at the position of air hole, γ_e is the specific weight of air, a is the sound velocity and then $\frac{2}{3} a$ is the mean velocity of air calculated under the assumption that the distribution of air velocity in the bearing clearance is parabolic. Assuming the air to expand adiabatically, the sound velocity and specific weight just after the air hole are to be given in the following formulas as $p_c=0.527\ p_0$,

$$\left.\begin{aligned} \gamma_e &= 0.775\ p_0{}^{1/1.4} , \\ a &= 310.3\ p_0{}^{1/7} , \end{aligned}\right\} \qquad (2)$$

where, p_0 in Kg/cm^2 (absolute pressure), γ_e in Kg/cm^3 and a in m/sec.

Then the equation (1) will be,

$$G = 1.007\ r_0 \cdot h \cdot p_0{}^{6/7} , \qquad (3)$$

where, r_0 and h are in mm, and G in g/sec.

Now adopting the state of non-eccentric rotation i. e. $h=\delta$ and giving the numerical values of δ and r_0, the equation (3) becomes,

$$G = 9.065\, p_0{}^{6/7} \times 10^{-2} . \qquad (4)$$

In the experiment, the quantity of flow was measured by pressure drop of air reservoir at intervals, taking very few pressure drops comparing the absolute pressure of air. The results of this experiment are plotted in Fig. 19 and the line in the diagram is the curve calculated from the equation (4). The experimental value is about the same as the theoretical value for $p_0=4.0\sim4.5\,\mathrm{Kg/cm^2}$ (gage pressure). This fact shows that non-eccentric rotating condition of bearing exists in this pressure range. This operating state of $p_0=4.0\sim4.5\,\mathrm{Kg/cm^2}$ corresponds to the state of minimum friction in which non-eccentric rotation exists. Accordingly the above assumption for the air flow just after the air hole is correct.

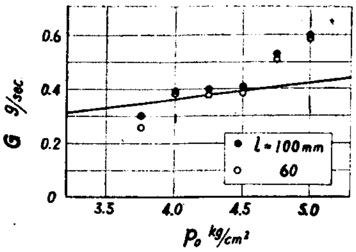

Fig. 19

From the fact that the state of minimum friction corresponds to the state of non-eccentric rotation, we can, therefore, explain the tendencies of μ_{min} in Fig. 11 and 12 as follows: Namely when we use Petroff's formula which corresponds to the following non-eccentric rotation

$$\mu = 2\pi^2\left(\frac{r}{\delta}\right)\left(\frac{\eta\cdot n}{q}\right), \qquad (5)$$

where, η=coefficient of viscosity, $q=\dfrac{W}{ld}$, it is made clear that μ_{min} in Fig. 11 takes the smallest value at $n=0$ and increases when the rotating speed rises, though actually μ_{min} does not become zero at $n=0$ owing to the surface irregularity of the bush and the shaft, and that μ_{min} in Fig. 12 increases with the decrease of the beaing clearance.

References

1) A. Kingsbury: Experiments with an Air-Lubricated Journal, Jour. Am. Soc. Naval Eng., Vol. 9, 1897.
2) W. J. Harrison: The Hydrodynamical Theory of Lubrication with Special Reference to Air as a Lubricant, Trans. Camb. Phil. Soc., Vol. 22, 1913.
3) R. Sasaki: Research on the Air Bearing, Kahei-Gakkaishi, Vol. 37, No. 1, 1943.